Bone Reports 14 (2021) 100739

Contents lists available at ScienceDirect

Bone Reports

journal homepage: www.elsevier.com/locate/bonr

Effect of ErhBMP-2-loaded β-tricalcium phosphate on ulna defects in the osteoporosis rabbit model

Tse-Yin Huang [a], Chang-Chin Wu [b,c,d], Pei-Wei Weng [e,f], Jian-Ming Chen [g,*], Weng-Ling Yeh [g,h]

[a] Ph.D. Program for Biotech Pharmaceutical Industry, School of Pharmacy, China Medical University, Taichung 40402, Taiwan
[b] Department of Orthopedics, National Taiwan University Hospital, College of Medicine, National Taiwan University, Taipei 10002, Taiwan
[c] Department of Biomedical Engineering, Yuanpei University of Medical Technology, Hsinchu 30015, Taiwan
[d] Department of Orthopedics, En Chu Kong Hospital, New Taipei City 23702, Taiwan
[e] Department of Orthopaedics, School of Medicine, College of Medicine, Taipei Medical University, Taiwan
[f] Department of Orthopaedics, Shuang Ho Hospital, Taipei Medical University, Taiwan
[g] Department of Orthopedic Surgery, Chang Gung Memorial Hospital-Linkou, Tao-Yuan 33305, Taiwan
[h] Bone and Joint Research Center, Chang Gung Memorial Hospital, Taoyuan, Taiwan

ARTICLE INFO

Keywords:
Ulna defect
Osteoporosis rabbit model
ErhBMP-2
Tricalcium phosphate

ABSTRACT

Purpose: Autografts, the gold standard treatment for large bone defects, present complications, especially in conditions with reduced bone-repair capacity, such as osteoporosis. *Escherichia coli*-derived recombinant human bone morphogenesis protein-2 (ErhBMP-2), was used in this study to improve the osteoinductivity of β-tricalcium phosphate (β-TCP). This study evaluated the bone-repair capacity of ErhBMP-2-loaded β-TCP on osteoporosis rabbit model, relative to the sole use of autograft and β-TCP treatments.

Methods: The osteoporosis rabbit model was induced through ovariectomy and glucocorticoid dosing; 2-cm segmental ulnar defects were created, which were treated with either autograft, β-TCP alone, or ErhBMP-2-loaded β-TCP or left untreated. The quality of newly formed ulnae was evaluated 8 weeks after ulnar surgery through micro-CT, biomechanical, histological, and histomorphometric assessments.

Results: The osteoporosis rabbit model was developed and maintained till the end of the study. The maximal load and stiffness in the ErhBMP-2-loaded TCP group were significantly higher than those in the autograft group, whereas the TCP-alone group performed similarly as did the untreated group in the force loading and stiffness tests. According to the micro-CT evaluation, the ErhBMP-2-loaded TCP group had significantly higher bone volume relative to the autograft and TCP-alone groups. Histological assessments revealed better defect bridging and marrow formation in the ErhBMP-2-loaded TCP group relative to the TCP-alone group. Mineral apposition rates were significantly higher in the ErhBMP-2-loaded TCP and autograft groups than in the TCP-alone and untreated groups.

Conclusion: Relative to autografts, ErhBMP-2-loaded TCP, as an alternative grafting material, provides better or comparable healing on critical-sized long bone defects in the osteoporosis rabbit model.

1. Introduction

Bone grafting is a common treatment for fractures or defects, especially those of critical size that cannot be self-repaired. Autografts are considered the gold standard treatment for large bone defects and theoretically possesses ideal clinical properties, including osteoinductivity, osteoconductivity, and osteogenicity (Calori et al., 2011). However, complications such as chronic pain, hematoma, fracture, muscle hernia, and nerve injury at the donor site have been reported (Goulet et al., 1997; Palmer et al., 2008). Other drawbacks of autografts include prolonged surgical time and a limited volume of available material (Chiarello et al., 2013). Moreover, health conditions characterized by reduced bone-repair capacities, such as aging or osteoporosis, may limit the application of autografts.

Abbreviations: BMC, bone mineral content; BMD, bone mineral density; BV, bone volume; β-TCP, β-tricalcium phosphate; ErhBMP-2, *Escherichia coli*-derived recombinant human bone morphogenesis protein-2; ROI, region of interest.

* Corresponding author at: Department of Orthopedic Surgery, Chang Gung Memorial Hospital-Linkou, Tao-Yuan 33305, Taiwan.
E-mail address: vantchen@gmail.com (J.-M. Chen).

https://doi.org/10.1016/j.bonr.2020.100739
Received 29 July 2020; Received in revised form 27 November 2020; Accepted 4 December 2020
Available online 10 December 2020
2352-1872/© 2020 The Authors. Published by Elsevier Inc. This is an open access article under the CC BY-NC-ND license (http://creativecommons.org/licenses/by-nc-nd/4.0/).

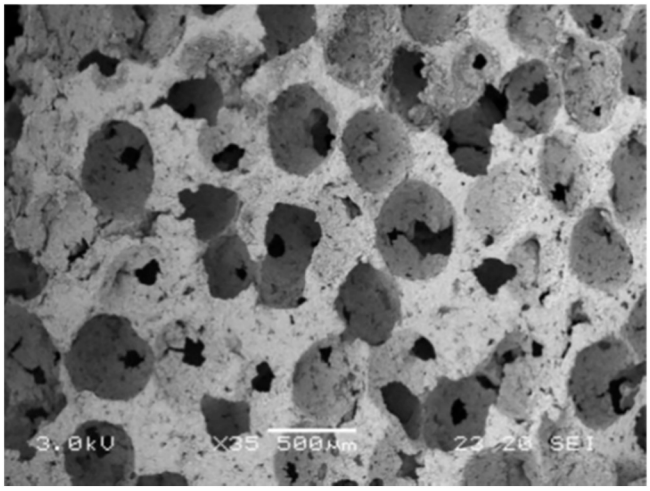

Fig. 1. Microstructure observation of β-TCP (Osteocera OC-G01) by scanning electron microscope.

Osteoporosis, a condition characterized by decreased bone mineral density (BMD) caused by menopause and aging (Anon, 2001), is related to reduced bone-repair abilities (Namkung-Matthai et al., 2001; Kubo et al., 1999), potentially leading to delayed healing and impaired outcomes of fractures and defects (Cheung et al., 2016). Delayed unions and nonunions were demonstrated to increase the health care cost (Hak et al., 2014) and the length of hospitalization stay, thereby leading to higher risks of complications. Furthermore, deteriorated microstructural qualities of osteoporotic bone were reported in a study (Xie et al., 2018), where such deterioration potentially reduces the bone regeneration effect of autografts. Consequently, alternative graft materials for osteoporotic patients are warranted.

Bone morphogenetic proteins (BMPs), a family of growth factors performing bioactivities in skeletal development, have been extensively investigated as osteoinducers for the treatment of fractures and defects (Lowery et al., 2018). In particular, BMP-2 and BMP-7 have been proven to induce osteoblastic differentiation from mesenchymal stem cells (Cheung et al., 2016); they are marketed as Infuse Bone Graft and OP-1, respectively, in the United States, for use in several orthopedic applications.

Tricalcium phosphate (TCP), especially β-TCP, has been widely used as a bone grafting material (Fillingham and Jacobs, 2016; Hernigou et al., 2017) because of its high porosity, biocompatibility, and bioconductivity (Abukawa et al., 2006; Chappard, 2017). Combinations of β-TCP and growth factors have been tested in several preclinical studies (Komaki et al., 2006; Szponder et al., 2018; Kim et al., 2017) and clinical trials (Tanaka et al., 2012; Comert Kilic et al., 2017; Huh et al., 2011).

Although numerous animal studies have investigated BMP-2 bioactivity in bone repair under healthy conditions, few studies have evaluated the osteoinductivity of BMP-2 in an osteoporosis model (Segredo-Morales et al., 2017). We hypothesized that a combination of BMP-2 and β-TCP is an alternative graft material for bone fractures and defects, especially in an osteoporosis animal model.

This study investigated the effect of *Escherichia coli*–derived recombinant human bone morphogenetic protein 2 (ErhBMP-2)-loaded β-TCP in critical-sized ulna defects in an osteoporosis rabbit model and compared it with the effects of autograft treatments and the sole use of β-TCP.

2. Methods

2.1. ErhBMP-2 and β-TCP granules

ErhBMP-2 was supplied by BioGend Therapeutics, Co. Ltd. (Taipei, Taiwan). The lyophilized cake was diluted with water for injection to a concentration of 0.125 mg/mL before use. β-TCP granules (Osteocera OC-G01, microstructure shown in Fig. 1) provided by Wiltrom Co. Ltd. (Taipei, Taiwan), had a diameter of 2–3 mm and a porosity of more than 70%. ErhBMP-2-loaded TCP was prepared by adding 160 μL of ErhBMP-2 solution into 200 mg of β-TCP granules and soaking for 15 min prior to implantation.

2.2. Animals and osteoporosis induction

The animal study was conducted by an AAALAC-accredited vivarium, PharmaLegacy Laboratories (Shanghai, China). A total of 10 female, 7-month-old New Zealand white rabbits were supplied by KangDa Rabbitry (Shangdong Province, China). The osteoporosis model was induced by following well-established methods through a combination of ovariectomy and glucocorticoid dosing (Sniekers et al., 2008; Permuy et al., 2019). Ovariectomy was conducted using the ventral abdominal approach. Briefly, the rabbits were anesthetized, and a longitudinal 4-cm incision was made in the midline of the lower abdominal area after the area was shaved, followed by ovary removal after clamping and ligation of the blood vessels of the pelvic funnel ligament, mesangial membrane, and intrinsic ligament of the ovary along the base of the ovary. After ovariectomy, glucocorticoid (i.m., 1 mg/kg, QD) was administered to all rabbits for 7 weeks, followed by 3 weeks of bodyweight restoration before the rabbits were operated on.

2.3. Densitometry

BMDs of the lumbar vertebral 2–5 and left femur were evaluated at 0, 8 and 18 week using dual-energy X-ray absorptiometry (Hologic, Discovery, USA) to ensure the osteoporosis animal model was induced.

2.4. Bilateral ulnar osteotomy surgery

Rabbits were operated on 10 weeks after ovariectomy and glucocorticoid dosing to establish an osteoporosis model. The animals were sedated using Zoletil (5 mg/kg, i.m.) and then transferred to isoflurane in oxygen anesthesia (0.5%–5%). The forelimbs were shaved, cleaned with 2% iodine tincture, and draped with sterile drapes. After skin preparation, each forelimb was incised in the upper-middle region on the inner aspect, and the ulna was exposed. Sections (2 cm) of the ulnar diaphysis were removed along with the periosteum by using a cutting saw to create segmental bone defects, which were then randomly filled with designated implant materials without fixation, namely 200 mg of TCP, 200 mg of ErhBMP-2-loaded (20 μg) TCP, autograft as a positive control or left empty without any implant materials as a negative control. Autograft was prepared by morselizing the bone removed from the ulna defect. Each group contained five samples.

2.5. Bone labeling

Tetracycline (20 mg/kg) and calcein (10 mg/kg) were administered with a 7 days gap twice as per the following routine: Tetracycline was administered 9 days prior to the start of the 4th week and 2 days prior to the start of the 8th week after osteotomy surgery. Calcein was administered 2 days prior to the start of the 4th week and 9 days prior to the start of the 8th week after osteotomy surgery.

2.6. Ulnar sample collection and biomechanical analysis

Ulnar samples were dissected free of flesh after humane euthanasia with CO_2 on the 56th day after surgery. The specimens containing the implant and the surrounding bone were trimmed using a water-cooled low speed saw and stored at −20 °C until further biomechanical tests.

Biomechanical tests (MTS 858, MTS system, USA) were conducted by inserting stainless steel rods through methylmethacrylate-potted

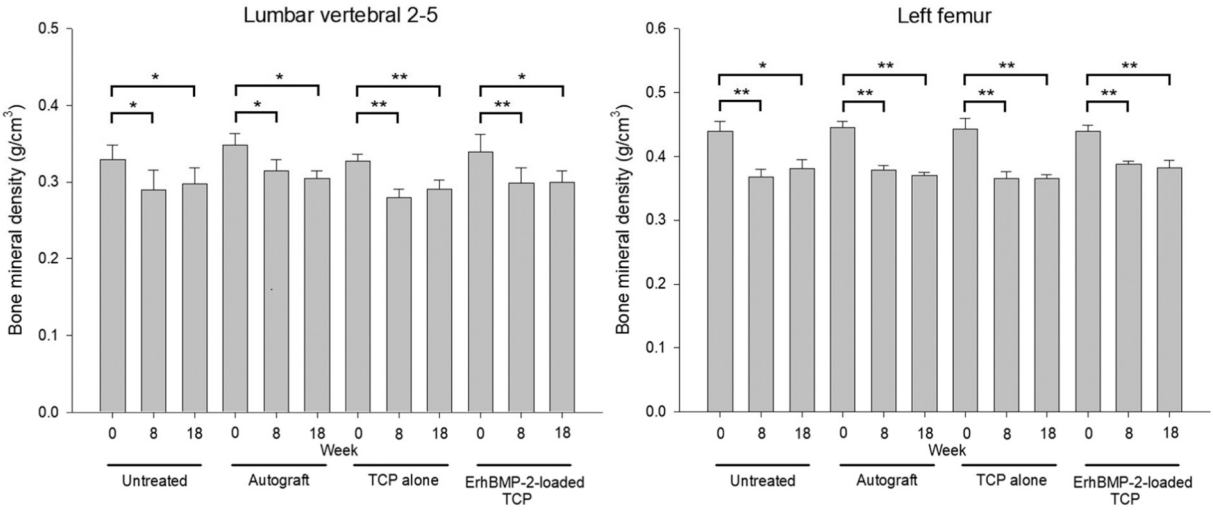

Fig. 2. Comparisons of bone mineral densities (mean ± S.E.) of lumbar vertebra 2–5 between week 0 (before the ovariectomy and glucocorticoid dosing), week 8 (after the ovariectomy and glucocorticoid dosing) and week 18 (the end of the study) (a) and those of the left femur between week 0, week 8 and week 18 (b). * $p < 0.05$, ** $p < 0.01$.

proximal and distal ends of the ulnae outside the defect region, where, for tensile strength, the rods were pulled no further once the peak force was reached.

Specimens remaining after the tensile test was fixed in 10% neutral buffer formalin for 48 h before being transferred to 70% methanol for further micro-CT scanning, undecalcified histology preparation, and histomorphometric analysis.

2.7. Micro-CT evaluation

Three-dimensional images were obtained for analysis of the bone structure and healing volume of the defect by using SkyScan-1176 (Bruker, Belgium) at a nominal isotropic resolution of 45 μm. The region of interest (ROI), a cylindrical volume with dimensions determined using microradiography, was used to investigate the center of the defect as well as the region between the biomaterial and bone interface. Bone volume (BV), bone mineral content (BMC), and bone mineral density (BMD) were determined through micro-CT.

2.8. Histology and histomorphometry

The explants remaining after micro-CT evaluation were dehydrated in an ascending alcohol series at room temperature by using a Shandon Excelsior™ Tissue Processor (Thermo-Fisher, China) before being embedded in methyl methacrylate. Two slabs (approximately 50 μm thick) were obtained for each specimen by using a saw and grinder from EXAKT (Germany). One of the slabs for each specimen was stained with toluidine blue (pH 6.5) for microscopic evaluation of healing activities; semiquantitative assessments were made on a 0–4 scale and included the assessment of defect bridging (the gap between the fractured ends, 0 for gap without filling and 4 for no gap left), marrow formation (hematopoietic space and fatty tissue formation within the new bone area, 0 for none and 4 for more than 75% of the new bone area), and implant material residual (amount of implanted materials left in the fractured gap, 0 for no degradation and 4 for complete removal).

The other slabs for each specimen were left unstained for histomorphometric analysis, wherein the mineral apposition and bone formation rates were measured using fluorochrome-labeled microscopy. Bone formation rates within the labeled periods in each treatment group were defined according to the American Society for Bone and Material

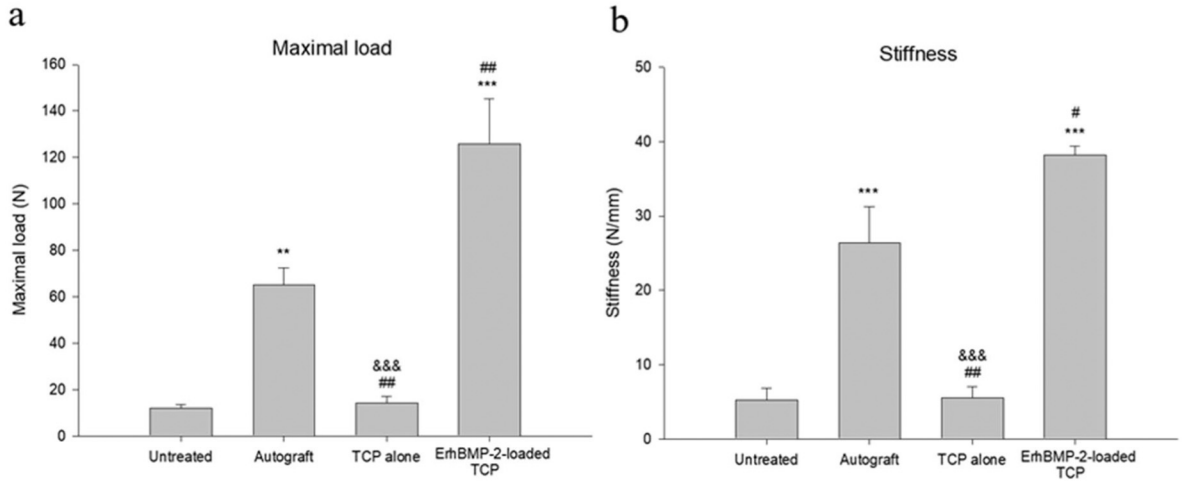

Fig. 3. (a) Mean (±S.E.) maximal load and (b) calculated stiffness in the biomechanical analysis. ** $p < 0.01$, *** $p < 0.001$, TCP alone, ErhBMP-2-loaded TCP, autograft vs. untreated. # $p < 0.05$, ## $p < 0.01$, TCP alone, ErhBMP-2-loaded TCP vs. autograft. &&& $p < 0.001$, TCP alone vs. ErhBMP-2-loaded TCP.

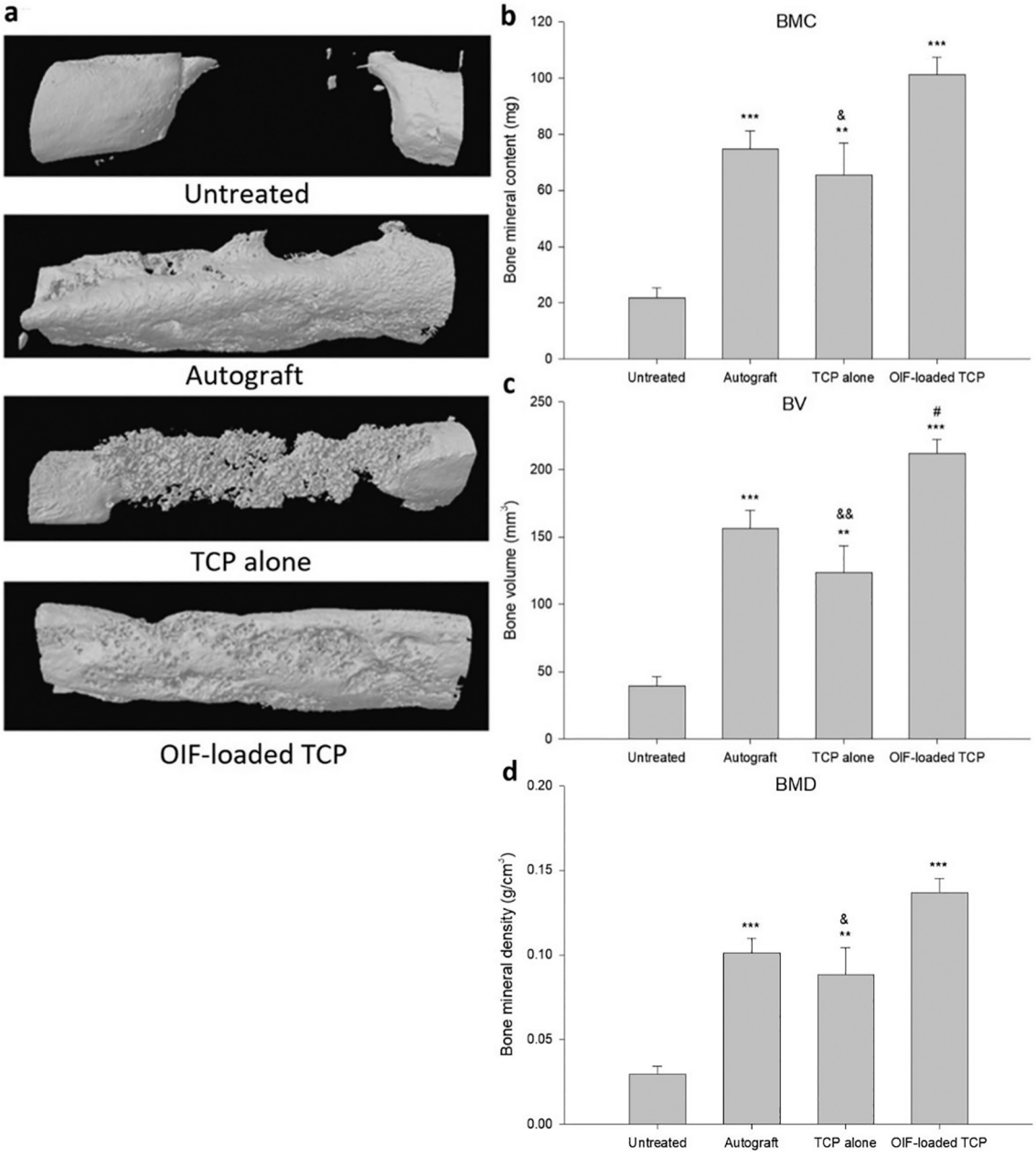

Fig. 4. (a) Representative micro-CT images in each treatment group; (b) mean (±S.E.) bone mineral content (BMC), (c) bone volume (BV), and (d) bone mineral density (BMD) in the ulna defect areas. ** $p < 0.01$, *** $p < 0.001$, ErhBMP-2-loaded TCP, autograft vs. untreated. # $p < 0.05$, ErhBMP-2-loaded TCP vs. autograft. & $p < 0.05$, && $p < 0.01$, TCP alone vs. ErhBMP-2-loaded TCP.

Research(ASBMR) Histomorphometry Nomenclature Committee (Dempster et al., 2013).

2.9. Statistical analysis

IBM® SPSS® Statistics 19 was used in statistical comparisons.

3. Results

3.1. Densitometry

The mean BMD in the lumbar vertebrae 2–5 (Fig. 2a) and the left femur (Fig. 2b) were significantly decreased in all rabbits after the ovariectomy and after 7 weeks of glucocorticoid dosing. Comparable BMD means in both LV2–5 and the left femur were found at the end of the 8th (after the induction of osteoporosis animal model) and 18th (at the end of the study) weeks, indicating that the low bone density condition was maintained in all rabbits during the ulna defect healing process.

3.2. Biomechanical analysis

The maximal load and stiffness results are depicted in Fig. 3a and b. The ErhBMP-2-loaded TCP and autograft groups performed better, with statistical significance, in the force loading and stiffness tests relative to the untreated group. The maximal load and stiffness in the ErhBMP-2-loaded TCP group were significantly higher than those in the autograft group, whereas the TCP-alone group performed similarly as did the untreated group in the force loading and stiffness tests.

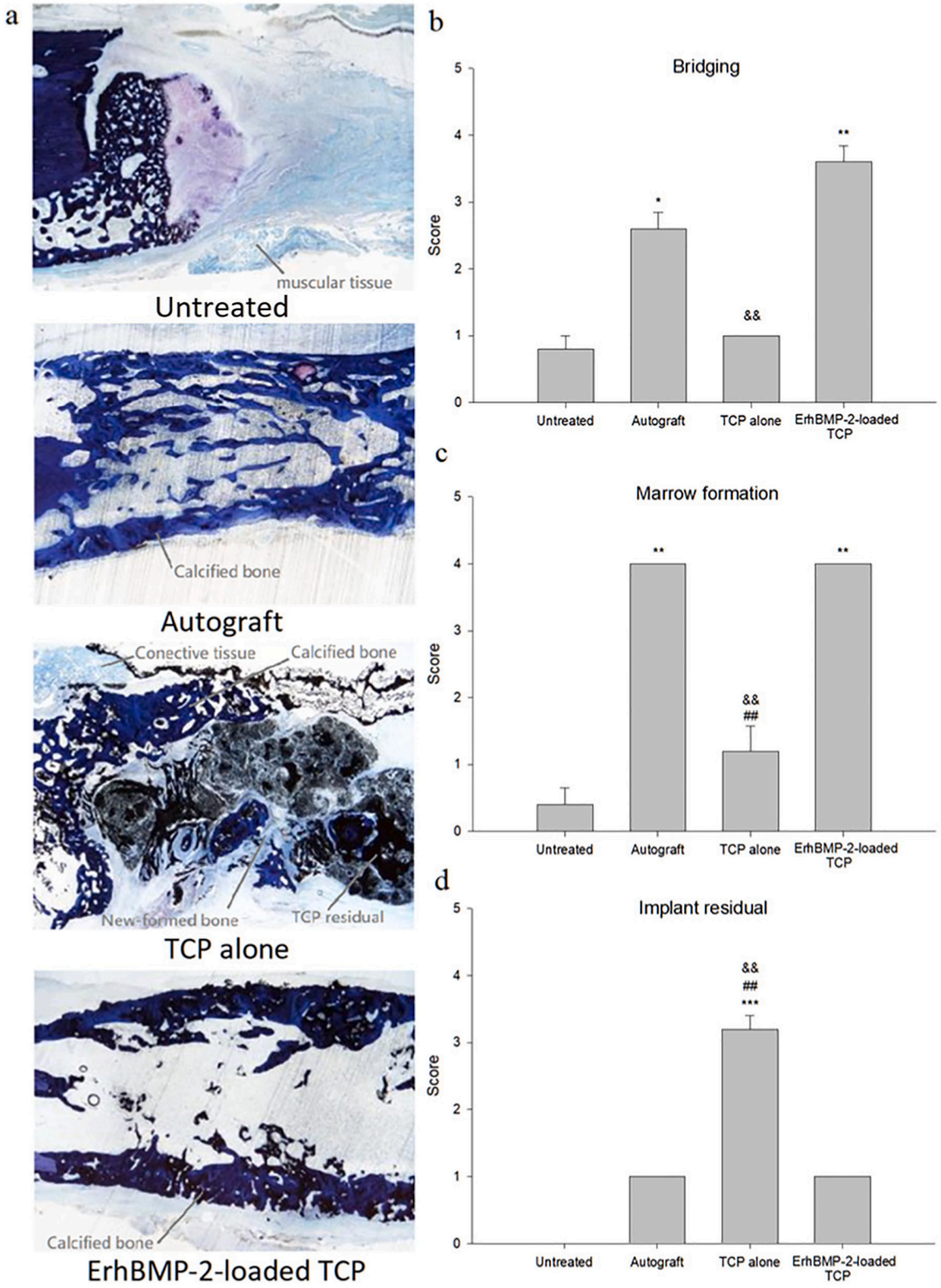

Fig. 5. (a) Representative histological section images of ulnae after each treatment; (b) mean (±S.E.) results of semiquantified analysis of defect recovery in bridging, (c) marrow formation, and (d) implant residual. * $p < 0.05$, ** $p < 0.01$, *** $p < 0.001$, TCP alone, ErhBMP-2-loaded TCP, autograft vs. untreated. ## $p < 0.01$, TCP alone vs. autograft. && $p < 0.01$, TCP alone vs. ErhBMP-2-loaded TCP.

3.3. Micro-CT evaluation

Representative micro-CT images in each treatment group are presented in Fig. 4a. The BMC, BV, and BMD of each group are illustrated in Fig. 4b-d. The BMC, BV, and BMD of the TCP-alone, ErhBMP-2-loaded TCP, and autograft groups were all significantly higher than those of the untreated group. Additionally, the BV of the ErhBMP-2-loaded TCP group was significantly higher than that of the autograft group, and the BMC in the ErhBMP-2-loaded TCP group was nonsignificantly higher ($p = 0.086$) than that in the autograft group.

Table 1
Row data of semiquantitative assessments of bridging, marrow formation, and implant residual for each sample.

Group	ID & site	Bridging	Marrow formation	Implant residual
Untreated	R1005-R	1	0	0
	R1006-L	1	1	0
	R1009-R	1	0	0
	R1013-R	0	0	0
	R1018-L	1	1	0
	Mean	0.8 ± 0.2	0.4 ± 0.2	0.0 ± 0.0
Autograft	R1006-R	3	4	1
	R1007-L	3	4	1
	R1011-L	3	4	1
	R1012-R	2	4	1
	R1022-L	2	4	1
	Mean	2.6 ± 0.2	4.0 ± 0.0	1 ± 0.0
TCP alone	R1007-R	1	0	3
	R1012-L	1	1	3
	R1013-L	1	2	4
	R1015-L	1	1	3
	R1018-R	1	2	3
	Mean	1.0 ± 0.0	1.2 ± 0.4	3.2 ± 0.2
ErhBMP-2-loaded TCP	R1005-L	4	4	1
	R1009-L	4	4	1
	R1011-R	3	4	1
	R1015-R	4	4	1
	R1022-R	3	4	1
	Mean	3.6 ± 0.2	4.0 ± 0.0	1.0 ± 0.0

3.4. Histology

Representative images of histological sections of specimens from each group are shown in Fig. 5a. The results of the histologic assessments of defect bridging, marrow formation, and implant material residuals of each treatment group are shown in Fig. 5b-d, with the row data attached in Table 1. The degrees of defect bridging and marrow formation in the ErhBMP-2-loaded TCP group were significantly higher than those in the TCP-alone and untreated groups. The degree of defect bridging in the autograft group was significantly higher than that in the untreated group. Marrow formation in the autograft group was significantly higher than that in the TCP-alone group. The implant material residual in the TCP-alone group was significantly higher than that in the ErhBMP-2-loaded TCP and autograft groups.

3.5. Histomorphometry

The mineral apposition rate and the bone formation rate in each treatment group are presented in Fig. 6a and b. The mineral apposition rates in defect areas in the ErhBMP-2-loaded TCP and autograft groups were significantly higher than those of rabbits in the TCP-alone and untreated groups. The bone formation rates in the TCP-alone, ErhBMP-2-loaded TCP, and autograft groups were significantly higher than that in the untreated group, with no significant difference among the three treatment groups.

4. Discussion

The present study compared the postoperative recovery and bone healing ability of segmental ulna defects in an osteoporosis animal model among TCP-alone, ErhBMP-2-loaded TCP, and autograft groups, with a defect-untreated group functioning as a negative control. The defect areas of the specimens in the untreated group did not spontaneously heal at the end of the study, confirming the influence of the critical size of ulna defects. In the microscopic assessment, histologic sections revealed comparable scoring in bridging and marrow formation in the ErhBMP-2-loaded TCP and autograft treatment groups. Relatively higher BMC and BV were discovered in the defect areas in the ErhBMP-2-loaded TCP treatment group than in the autograft treatment group. Results of the biomechanical analysis indicated that the ErhBMP-2-loaded TCP group had the stiffest new bone.

Rabbits are promising as a model of osteoporosis research because of their suitable size and as well as the feasibility of Haversian remodeling and closure of the epiphyseal plate (Permuy et al., 2019). The BMD of rabbits significantly decreased after osteoporosis induction and was maintained till the end of the study.

Regarding wound healing after implantation of materials containing BMP-2, although acute edema related to BMP-2 was reported (Benglis et al., 2008) and observed in a case report (Merrick et al., 2013), no significant difference was found in postoperative forelimb edema measurement among the treatment groups. The degree of edema in each group reached the peak values within 10 days after osteotomy surgery and was gradually resolved over time (data not shown).

The biomechanical analysis further confirmed an improvement in

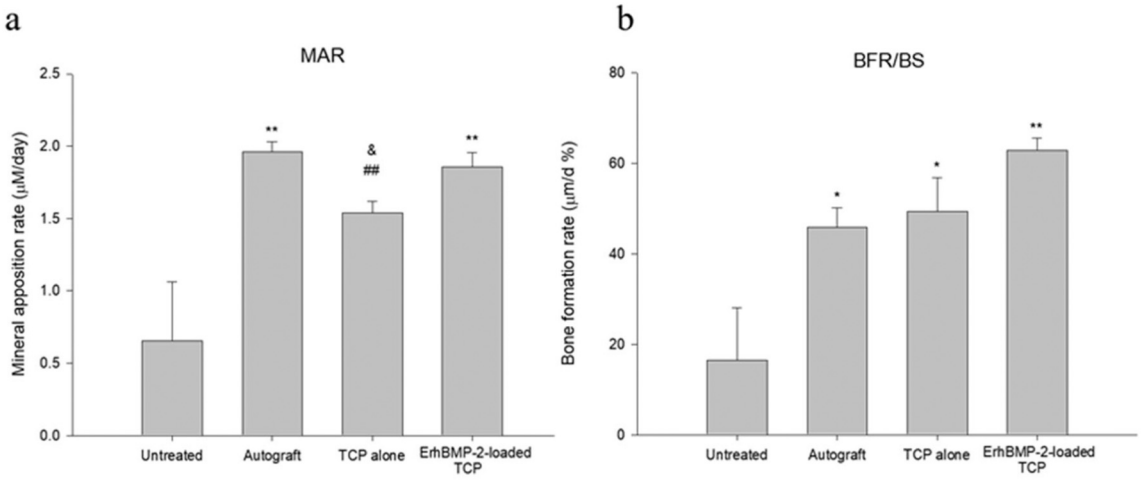

Fig. 6. (a) Mean (±S.E.) mineral apposition rate (MAR) and (b) bone formation rate (BFR/BS) of each treatment. * $p < 0.05$, ** $p < 0.01$, TCP alone, ErhBMP-2-loaded TCP, autograft vs. untreated. ## $p < 0.01$, TCP alone vs. autograft. & $p < 0.05$, TCP alone vs. ErhBMP-2-loaded TCP.

ErhBMP-2-induced bone regeneration on TCP. The performance in the force-loading examination was comparable between the TCP-alone and untreated groups, implying that TCP implantation alone could not generate the linkage between the defect area within 8 weeks, whereas the addition of ErhBMP-2 to TCP strongly improved the stiffness of the newly formed bone, which was significantly stiffer than the new bone formed after autograft treatment. In addition, data of the micro-CT scan support the results of the biomechanical evaluation. The BV and BMC of the bone regenerated by ErhBMP-2-loaded TCP were the highest among all treatment groups.

Regarding the microenvironment of the regenerated bone, different components were observed in the histology sections for each treatment. Numerous TCP particles were left in the specimens of the TCP-alone treatment group. By contrast, few TCP granules were left in the defect areas of specimens of the ErhBMP-2-loaded TCP group, which were attributable to the strong resorptive effect of BMP-2 on β-TCP (Kitasato et al., 2019). Furthermore, massive calcified bones were observed in the specimens of the ErhBMP-2-loaded TCP treatment group, verifying the osteoinductivity of BMP-2. Semi-quantified scoring indicated the detailed differences among the treatment groups. Of the five ErhBMP-2-loaded TCP-treated samples, three had a score of 4 in bridging assessment, whereas none of the autografted samples had a score of 4 in bridging, although the means between the groups were not significantly different. Similar trends were observed for the bone formation rate calculated using dye-labeled bands. The bone formation rate in the ErhBMP-2-loaded TCP treatment group was the highest among all treatment groups, although it did not significantly differ from that in the autograft treatment group ($p = 0.072$).

The applications of BMP-2 in the treatment of fractures or defects have been extensively reported in animal studies. However, little is known regarding the osteoinductivity of BMP-2, particularly in osteoporotic conditions (Segredo-Morales et al., 2017). Downregulated genes or mRNA of BMP-2 have been reported in senile animals with osteopenia (Fleet et al., 1996; Matsumoto et al., 2001) and ovariectomized osteoporotic mice (Zhou et al., 2001), thereby indicating a link between the dysregulation of BMP-2 and poor bone recovery abilities in osteoporosis. Consequently, a combination of BMP-2 and TCP may compensate for the deficiency in local growth factor, providing better outcomes relative to not only autograft treatment but also the sole use of TCP implantation. In addition, the resorptive effect induced by BMP-2 on TCP may synergistically accelerate bone remodeling in defect areas.

In conclusion, relative to autografts, ErhBMP-2-loaded TCP, as an alternative grafting material, provides better or comparable healing on critical-sized long bone defects in our animal model of osteoporosis.

Funding

The authors received no specific funding for this work.

CRediT authorship contribution statement

Tse-Yin Huang: Methodology, Formal analysis, Writing - Original Draft. **Chang-Chin Wu**: Writing- Reviewing and Editing. **Pei-Wei Weng**: Writing- Reviewing and Editing. **Jian-Ming Chen**: Conceptualization, Validation, Writing - Review & Editing. **Weng-Ling Yeh**: Supervision, Writing- Reviewing and Editing.

Declaration of competing interest

The authors have declared no conflict of interest.

Acknowledgments

We extend our appreciation to Wiltrom Co. Ltd. and BioGend Therapeutics, Co. Ltd. for their supply of β-TCP and ErhBMP-2, respectively. This manuscript was edited by Wallace Academic Editing.

References

Abukawa, H., et al., 2006. The engineering of craniofacial tissues in the laboratory: a review of biomaterials for scaffolds and implant coatings. Dent. Clin. N. Am. 50 (2), 205–216 (viii).

Anon *Osteoporosis prevention, diagnosis, and therapy.* Jama, 2001. **285**(6): p. 785–95.

Benglis, D., M.Y. Wang, and A.D. Levi, *A comprehensive review of the safety profile of bone morphogenetic protein in spine surgery.* Neurosurgery, 2008. 62(5 Suppl 2): p. ONS423–31; discussion ONS431.

Calori, G.M., et al., 2011. The use of bone-graft substitutes in large bone defects: any specific needs? Injury 42 (Suppl. 2), S56–S63.

Chappard, D., 2017. Beta-tricalcium phosphate and bone surgery: editorial. Morphologie 101 (334), 111–112.

Cheung, W.H., et al., 2016. Fracture healing in osteoporotic bone. Injury 47 (Suppl. 2), S21–S26.

Chiarello, E., et al., 2013. Autograft, allograft and bone substitutes in reconstructive orthopedic surgery. Aging Clin. Exp. Res. 25 (Suppl. 1), S101–S103.

Comert Kilic, S., Gungormus, M., Parlak, S.N., 2017. Histologic and histomorphometric assessment of sinus-floor augmentation with beta-tricalcium phosphate alone or in combination with pure-platelet-rich plasma or platelet-rich fibrin: a randomized clinical trial. Clin. Implant. Dent. Relat. Res. 19 (5), 959–967.

Dempster, D.W., et al., 2013. Standardized nomenclature, symbols, and units for bone histomorphometry: a 2012 update of the report of the ASBMR histomorphometry nomenclature committee. J. Bone Miner. Res. 28 (1), 2–17.

Fillingham, Y. and J. Jacobs, *Bone grafts and their substitutes.* Bone Joint J, 2016. **98-b**(1 Suppl A): p. 6–9.

Fleet, J.C., et al., 1996. The effects of aging on the bone inductive activity of recombinant human bone morphogenetic protein-2. Endocrinology 137 (11), 4605–4610.

Goulet, J.A., et al., 1997. Autogenous iliac crest bone graft. *Complications and functional assessment.* Clin Orthop Relat Res 339, 76–81.

Hak, D.J., et al., 2014. Delayed union and nonunions: epidemiology, clinical issues, and financial aspects. Injury 45 (Suppl. 2), S3–S7.

Hernigou, P., et al., 2017. Beta-tricalcium phosphate for orthopedic reconstructions as an alternative to autogenous bone graft. Morphologie 101 (334), 173–179.

Huh, J.B., et al., 2011. Randomized clinical trial on the efficacy of Escherichia coli-derived rhBMP-2 with beta-TCP/HA in extraction socket. J Adv Prosthodont 3 (3), 161–165.

Kim, C.H., Ju, M.H., Kim, B.J., 2017. Comparison of recombinant human bone morphogenetic protein-2-infused absorbable collagen sponge, recombinant human bone morphogenetic protein-2-coated tricalcium phosphate, and platelet-rich fibrin-mixed tricalcium phosphate for sinus augmentation in rabbits. J Dent Sci 12 (3), 205–212.

Kitasato, S., et al., 2019. Local application of alendronate controls bone formation and beta-tricalcium phosphate resorption induced by recombinant human bone morphogenetic protein-2. J. Biomed. Mater. Res. A 108 (3), 528–536.

Komaki, H., et al., 2006. Repair of segmental bone defects in rabbit tibiae using a complex of beta-tricalcium phosphate, type I collagen, and fibroblast growth factor-2. Biomaterials 27 (29), 5118–5126.

Kubo, T., et al., 1999. Osteoporosis influences the late period of fracture healing in a rat model prepared by ovariectomy and low calcium diet. J. Steroid Biochem. Mol. Biol. 68 (5–6), 197–202.

Lowery, J.W., Rosen, V., Approaches, Bone Morphogenetic Protein-Based Therapeutic, 2018. Cold Spring Harb. Perspect. Biol. 10(4).

Matsumoto, A., et al., 2001. Effect of aging on bone formation induced by recombinant human bone morphogenetic protein-2 combined with fibrous collagen membranes at subperiosteal sites. J. Periodontal Res. 36 (3), 175–182.

Merrick, M.T., Hamilton, K.D., Russo, S.S., 2013. Acute epidural lipedema: a novel entity and potential complication of bone morphogenetic protein use in lumbar spine fusion. Spine J. 13 (10), e15–e19.

Namkung-Matthai, H., et al., 2001. Osteoporosis influences the early period of fracture healing in a rat osteoporotic model. Bone 28 (1), 80–86.

Palmer, W., Crawford-Sykes, A., Rose, R.E., 2008. Donor site morbidity following iliac crest bone graft. West Indian Med J 57 (5), 490–492.

Permuy, M., et al., 2019. Rabbit as model for osteoporosis research. J. Bone Miner. Metab. 37 (4), 573–583.

Segredo-Morales, E., et al., 2017. BMP delivery systems for bone regeneration: Healthy vs osteoporotic population. *Review.* J Drug Deliv Sci Technol.

Sniekers, Y.H., et al., 2008. Animal models for osteoarthritis: the effect of ovariectomy and estrogen treatment - a systematic approach. Osteoarthr. Cartil. 16 (5), 533–541.

Szponder, T., et al., 2018. Application of platelet-rich plasma and tricalcium phosphate in the treatment of comminuted fractures in animals. In Vivo 32 (6), 1449–1455.

Tanaka, T., et al., 2012. Use of an injectable complex of beta-tricalcium phosphate granules, hyaluronate, and fibroblast growth Factor-2 on repair of unstable intertrochanteric fractures. Open Biomed Eng J 6, 98–103.

Xie, F., et al., 2018. Microstructural properties of trabecular bone autografts: comparison of men and women with and without osteoporosis. Arch. Osteoporos. 13 (1), 18.

Zhou, S., et al., *Estrogen modulates estrogen receptor alpha and beta expression, osteogenic activity, and apoptosis in mesenchymal stem cells (MSCs) of osteoporotic mice.* J Cell Biochem Suppl, 2001. **Suppl 36**: p. 144–55.